Histochem Cell Biol (2005) 123: 613–620
DOI 10.1007/s00418-004-0750-5

ORIGINAL PAPER

Martin Westermann · Frank Steiniger · Walter Richter

Belt-like localisation of caveolin in deep caveolae and its re-distribution after cholesterol depletion

Accepted: 22 November 2004 / Published online: 12 May 2005

Abstract Caveolae are specialised vesicular microdomains of the plasma membrane. Using freeze-fracture immunogold labelling and stereoscopic imaging, the distribution of labelled caveolin 1 in caveolae of 3T3-L1 mouse fibroblast cells was shown. Immunogold-labelled caveolin structures surrounded the basolateral region of deeply invaginated caveolae like a belt whereas in the apical region distal to the plasma membrane, the caveolin labelling was nearly absent. Shallow caveolar membranes showed a dispersed caveolin labelling. After membrane cholesterol reduction by methyl-ß-cyclodextrin treatment, a dynamic re-distribution of labelled caveolin 1 and a flattening of caveolar structures was found. The highly curved caveolar membrane got totally flat, and the initial belt-like caveolin labelling disintegrated to a ring-like structure and later to a dispersed order. Intramembrane particle-free domains were still observable after cholesterol depletion and caveolin re-distribution. These results indicate that cholesterol interacting with caveolin structures at the basolateral part of caveolae is necessary for the maintenance of the deeply invaginated caveolar membranes.

Keywords Caveolin · Caveolae · Freeze-fracture immunolabelling · Cholesterol depletion · Stereoscopic imaging

Introduction

Caveolae are invaginations of the plasma membrane with a round flask shape and a diameter in the range of 50–100 nm (Yamada 1955). Caveolae are present in most animal cell types. They are abundant in fibroblasts, adipocytes, type 1 pneumocytes, endothelial cells and smooth and striated muscle cells (Couet et al. 1997). They are attached to the plasma membrane via a short caveolar neck, but they may also appear as shallow pits (Severs 1988). Many different cellular functions are attributed to caveolae, such as cell-surface signal-transduction, mechano-transduction, potocytosis, endocytosis and intracellular cholesterol transport (for reviews, see Parton 1996; Anderson 1998; Simons and Toomre 2000; Stan 2002). In electron microscopical studies, caveolae appear as more or less static invaginations of the plasma membrane. Studies in endothelial cells (Schnitzer et al. 1994) and fibroblasts (Parton et al. 1994) showed that caveolae are dynamic structures (Kurzchalia and Parton 1996). They can bud from the plasma membrane, and their internalisation is regulated by the molecular transport machinery of vesicle budding, docking and fusion (Schnitzer et al. 1995; Schnitzer et al. 1996). Caveolae contain special lipids, such as phosphoinositides (Hope and Pike 1986) and gangliosides (Montesano et al. 1982; Parton 1994). It has been shown that the plasmatic surface of caveolae is covered by a characteristic "striated coat" formed by filamentous structures in a spiral arrangement (Peters et al. 1985; Rothberg et al. 1992). It is supposed that the protein caveolin is a structural component of the caveolar "coat" (Rothberg et al. 1992).

Caveolin is an integral membrane protein of 21–23 kDa (Kurzchalia et al. 1992). It can be palmitoylated on multiple cysteine residues (Dietzen et al. 1995) and binds cholesterol (Murata et al. 1995). Caveolin forms a hairpin-like structure in the membrane with amino and carboxyl termini on the cytoplasmatic side flanked by a hydrophobic intramembrane domain (Dupree et al. 1993; Monier et al. 1995). A sequence of amino acids called the scaffolding domain interacts with many signalling proteins (Li et al. 1996). In vivo, caveolin has a homo-oligomeric structure. It forms high molecular mass complexes (350–400 kDa; Monier et al. 1995; Sargiacomo et al. 1995) and is insoluble in non-ionic

M. Westermann (✉) · F. Steiniger · W. Richter
Elektronenmikroskopisches Zentrum am Klinikum der Friedrich-Schiller-Universität Jena,
Ziegelmühlenweg 1, 07740, Jena, Germany
E-mail: martin.westermann@uni-jena.de
Tel.: +49-3641-933123
Fax: +49-3641-933102

detergents such as Triton X-100 (Kurzchalia et al. 1992). The expression of caveolin 1 in caveolin-free lymphocytes leads to de novo formation of caveolae (Fra et al. 1995). These findings suggest that caveolin is necessary for the structure and function of caveolae.

It has been shown that cyclodextrins [ß-cyclodextrin and methyl-ß-cyclodextrin (MßCD)] remove cholesterol from cultured cells (Ohtani et al. 1989; Klein et al. 1995). We used MßCD because it was found to be more efficient than ß-cyclodextrin (Klein et al. 1995). Cyclodextrins are cyclic glucose oligomers that have the ability to include lipophilic substances in their pores; MßCD, in particular, forms water-soluble inclusion complexes with cholesterol (Pitha et al. 1988; Irie et al. 1992).

In the present study, we localised caveolin 1 by freeze-fracture electron microscopy using the SDS freeze-fracture immunogold-labelling technique (Fujimoto 1995) and stereoscopic interpretation. We analysed the effect of cholesterol depletion on the caveolar structure and showed a re-distribution of caveolin 1 in the plasma membrane.

Materials and methods

Cells and cell culture

In order to examine a cell line with high numbers of caveolae, 3T3-L1 mouse fibroblasts were grown to confluence at 37°C and 10% CO_2 in DMEM (Dulbecco's modified Eagle's medium) containing 10% bovine serum. Three cell culture dishes were prepared per experiment. One culture was directly prepared for the freeze-fracture procedure, the second was incubated for 15 min and the third for 30 min with 15 mM MßCD in serum-free culture medium. Then, the cells were washed with phosphate-buffered saline (PBS, 75 mM NaCl, 12.5 mM NaH_2PO_4, 67 mM Na_2HPO_4, pH 7.2) and physically fixed by rapid freezing.

Electron microscopy

Freeze-fracture preparation

Confluently grown 3T3-L1 fibroblast cells were washed twice with PBS at growth temperature and carefully abraded from the culture dishes. Aliquots of the chemically unfixed cell suspension were enclosed between two 0.1-mm thick copper profiles, as used for the sandwich double-replica technique. The sandwiches were physically fixed by rapid plunge freezing in liquid ethane/propane mixture cooled by liquid nitrogen. Freeze fracturing was performed in a BAF400T freeze-fracture unit (BAL-TEC, Liechtenstein) at −150°C using a double-replica stage. The fractured samples were shadowed without etching with 2–2.5 nm platinum/carbon (Pt/C) at an angle of 35°. The evaporation of Pt/C with electron guns was controlled by a thin-layer quartz crystal monitor.

Freeze-fracture immunogold labelling of caveolin

For freeze-fracture immunogold labelling and subsequent electron microscopy, the freeze-fracture replicas were transferred to a "digesting" solution (2.5% SDS in 10 mM Tris buffer pH 8.3 and 30 mM sucrose) and incubated overnight according to Fujimoto (1997). The replicas were washed four times in PBS to remove SDS and treated for 30 min with PBS +1% BSA (bovine serum albumin), then they were placed on a drop of an 1:50 diluted solution of the anti-caveolin 1 antibody (polyclonal rabbit IgG, Santa Cruz Biotechnologies, Santa Cruz, USA) in PBS with 0.5% BSA for 1 h. The replicas were washed subsequently four times with PBS and placed on an 1:50 diluted solution of the second gold-conjugated antibody (goat anti-rabbit IgG with 10 nm gold, British Biocell International, Cardiff, UK) in PBS with 0.5% BSA for 1 h. After immunogold labelling, the replicas were immediately rinsed several times in PBS, fixed with 0.5% glutaraldehyde in PBS for 10 min at room temperature, washed four times in distilled water and finally picked onto Formvar-coated grids for viewing in an EM 902 A electron microscope (Zeiss, Oberkochen, Germany) or a Philips-CM 120 electron microscope (Philips, the Netherlands). Freeze-fracture micrographs were preferentially mounted with the direction of the platinum shadowing from bottom up.

Stereoscopic imaging

Stereo pairs and tilt series of samples were taken with a tiltable Gatan 626-DH cryo holder (Gatan GmbH Munich, Germany). For stereoscopic views, a tilt angle of 5° was set. For tilt series, a sequence of micrographs of up to 22 in steps of 5° were taken with a FastScan-CCD-Camera 1,024×1,024 (TVIPS GmbH, Munich, Germany). The image shift of the stereo pairs was calculated by means of cross-correlation using the software EMMENU V.3.Q (TVIPS GmbH). The two micrographs of a stereo pair were mounted with a tilt angle of 5° using the software 3D-FotoStudio 1.2 (M. Filkorn Software, Germany).

Results

The distribution of caveolin 1 in 3T3-L1 mouse fibroblast cells was analysed using freeze-fracture replica immunolabelling (Fujimoto 1997). This method is an extension of the freeze-fracture electron microscopy. It allows the in situ visualisation of molecular composition and characteristics of biomembranes. Performing the detergent-digestion freeze-fracture labelling procedure, chemically unfixed 3T3-L1 cells were rapidly cryofixed and then freeze fractured. The fracture plane was physically stabilised by evaporated Pt/C (replica). The replicas were cleaned from cellular components by SDS-detergent digestion (Fujimoto 1997) whereas biomolecules that were in direct (i.e. "adsorptive") contact with

the Pt/C replica film, like membrane lipids and membrane-bound proteins, were kept bound at the replica. After re-naturation, the replica-bound membrane molecules can be immunolabelled (Takizawa and Robinson 2000).

Figure 1 shows a non-stereoscopic freeze-fracture view of the protoplasmic fracture face (PF) of the plasma membrane of 3T3-L1 mouse fibroblast cells after immunolabelling of caveolin 1. These cells were not treated with MßCD and were rapidly frozen in a chemically unfixed state. The caveolae are not randomly distributed on the plasma membrane of the fibroblast cells; they are clustered in distinct membrane patches. In confluently grown 3T3-L1 fibroblast cells, the number of caveolae in a patch of caveolae varied between 10 and 200, with densities of 15–22 caveolae/μm^2 .

On freeze fractures of the PF of the plasma membrane, caveolae normally appear as round, invaginated pits with diameters between 60 nm and 80 nm (Fig. 1, arrows). The freeze-fracture micrograph in Fig. 1 is mounted with the direction of the platinum shadowing (35° angle) from bottom up so that the dark-appearing platinum decoration is found at the upper side of the caveolar pits (Fig. 1; arrows, Fig. 4). The bottom of deeply invaginated caveolar structures appears white because of the absence of platinum decoration. When the deeply invaginated caveolar membranes are not fractured out, the fracture plane crosses the ice of the caveolar pori (Fig. 1, arrowheads). In some cases, the caveolae do not appear as deeply invaginated structures but as shallow pits (Fig. 1, asterisks).

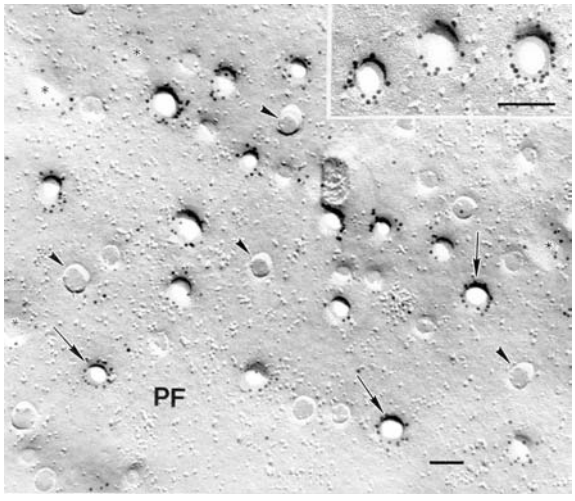

Fig. 1 Non-stereoscopic freeze-fracture micrograph of plasma membrane caveolae in chemically unfixed 3T3-L1 mouse fibroblast cells. The protoplasmic fracture face (*PF*) is immunolabelled with caveolin-1 antibody. Caveolae appear as round deep membrane depressions with diameters between 60 nm and 80 nm (*arrows*). The gold-labelled caveolin-1 molecules are found in ring-like structures surrounding the deeply invaginated caveolar pits (*arrows* and *inset*). When the caveolar membrane is not fractured, no label can be found at the remaining structures (*arrowheads*). A dispersed caveolin label is also found on shallow caveolar structures (*asterisks*). The shallow caveolae are nearly free of intramembrane protein particles; they have diameters between 80 nm and 110 nm. *Bars*: 100 nm

The 10-nm gold particles indicate immunolabelled caveolin-1 molecules. The density of gold particles within a cluster of caveolae was 112 ± 21 particles per micrometre squared counted on six different areas. The gold label surrounds the deep caveolar invaginations in a ring-like arrangement (Fig. 1, arrows and inset). In cases when the highly curved caveolar membrane is not split (Fig.1, arrowheads), no caveolin labelling can be found at the plasma membrane bordering the cross-fractured caveolar pori. It is remarkable that the dimensions of these cross-fractured pori in the case of unfixed cells (up to 80-nm diameter) are in the range of caveolar bulbs. A dispersed caveolin labelling is found on shallow caveolar structures having larger diameters (80–110 nm) than deeply invaginated caveolae (60–80 nm) (Fig. 1, asterisks). Observing the membrane (PF-fracture face) of the shallow caveolae, it is striking that these domains are almost free of intramembrane protein particles.

Figure 2 shows four stereoscopic images (5° tilt) of caveolae with immunolabelled caveolin 1. For better visualisation, the stereo images were mounted in a way that caveolae appear as elevations. In stereoscopic view, it is clearly observable that whole caveolar vesicles are replicated and stabilised only by the carbon layer. The stereoscopic views of deeply invaginated caveolae (Fig. 2a–c) show that most of the label is located like a belt in different heights at the basolateral region of the caveolae, with an increased density proximal to the bulk plasma membrane. The apical parts of the caveolar vesicles distal to the plasma membrane almost lack caveolin-1 labelling. The stereoscopic view of shallow caveolae (Fig. 2d) exhibits a dispersed caveolin labelling located in one level on the replicated membrane. Some single gold particles could be determined as a "false-positive" labelling (Rash and Yasumura 1999); they are adsorbed at the wrong side of the replica film (white arrows in Fig. 2a, b, d). Rough estimations of false-positive to positive located gold grains (signal:noise) resulted in 1–5 false-positive gold particles per hundred. Detail views of a densely labelled caveola (about 20 gold particles) are given in Fig. 3. Figure 3a and c again clearly show that the whole caveolar bulb is replicated and stabilised by the carbon layer. In order to visualise the spatial arrangement of the caveolin-1 labelling, the replica of one and the same caveola was tilted in the electron microscope from $-55°$ to $+55°$ inclination. The tilt series exhibits a caveolin-1 labelling surrounding the basolateral region of the caveola whereas the apical region indicated by the black arrow is free of caveolin-1 labelling. In Fig. 4, we try to summarise the structural data of the stereo and tilt analysis in a model for a deep, invaginated, caveolin-1 freeze-fracture immunolabelled caveola.

In order to analyse the caveolin distribution in cells after cholesterol depletion, we added 15 mM MßCD to serum-free culture medium for 15 min. Figure 5 shows a freeze-fracture micrograph of the PF with a cluster of

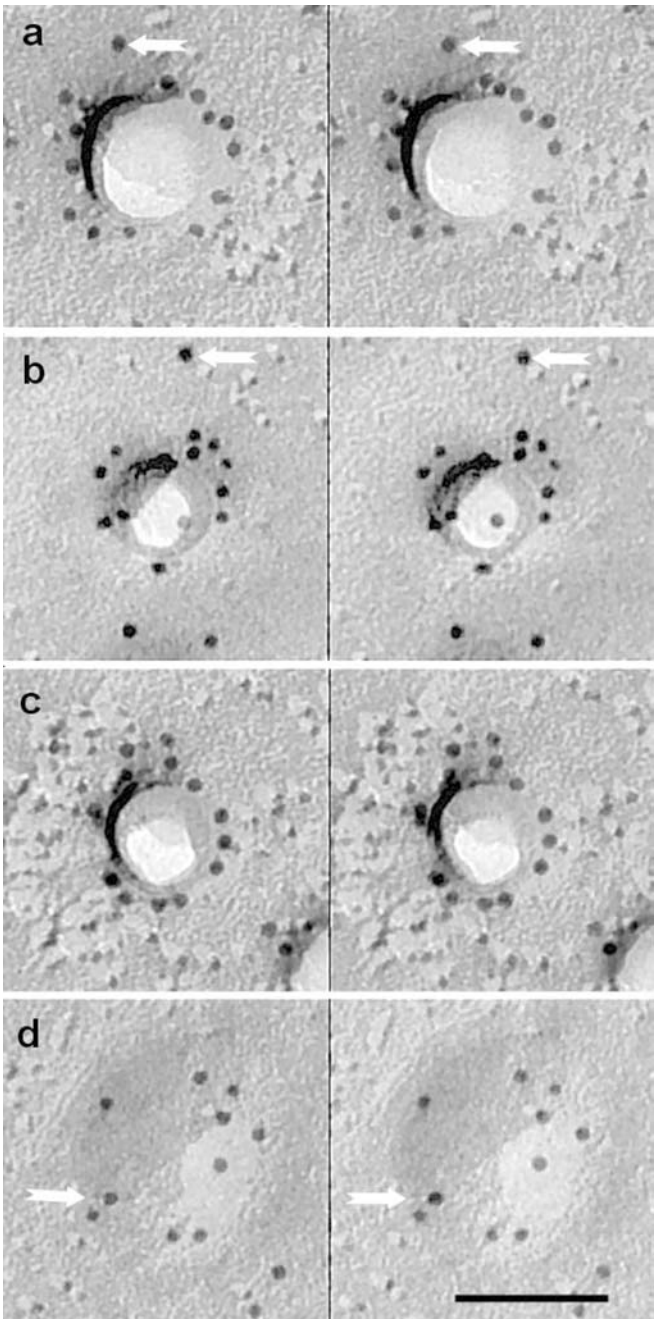

Fig. 2 Stereoscopic images of caveolae with immunolabelled caveolin 1 on the protoplasmic fracture face (PF) of 3T3-L1 mouse fibroblast cells. Stereo pairs of micrographs were taken with tilt angles of 5°. The stereo pairs in **a**, **b** and **c** show the distribution of caveolin 1 in deeply invaginated caveolae; the stereo pair in **d** shows that distribution in a shallow caveola. The images are mounted in such a way that caveolae appear as elevations. Deeply invaginated caveolae (**a**, **b**, **c**) are labelled mostly at basolateral levels whereas apical levels are nearly free of gold labelling. Shallow caveolae (**d**) are labelled in one height level on the replicated membrane. False-positive labelling is indicated by *white arrows* (**a, b, d**). *Bar*: 100 nm

plasma membrane caveolae in a 3T3-L1 fibroblast cell. Already after 15 min of cholesterol depletion, the shape of the caveolae in the 3T3-L1 cells changes dramatically. No deeply invaginated caveolar pit with high membrane curvature can be detected. All the caveolar membranes are flattened to shallow pits (Fig. 5, arrows), and the diameter of the caveolar structures increased from 60 nm to 80 nm for the deep caveolae to 80–110 nm for the flattened caveolae. Caused by the change of the caveolar shape, no cross-fractures through caveolar openings occur. The arrangement of gold particles indicating the distribution of caveolin molecules changes from distinct rings or belts at the basolateral region of deep caveolae to open circles or more dispersed rings in one height level at the periphery of the flattened caveolae (Fig. 5, arrows and inset). After 15 min MßCD treatment, the density of gold particles within a cluster of caveolae is 108 ± 18 particles per micrometre squared counted on six different areas. Looking at the intramembrane particle distribution, it can be seen that the central parts of the flattened caveolae are almost free of intramembrane protein particles.

Figure 6 shows the results of a freeze-fracture immunogold labelling of caveolin 1 after 30 min of cholesterol depletion by MßCD. The caveolar domain structures on the PF of the plasma membrane have disappeared and the membrane looks nearly flat whereas gold particles indicating immunolabelled caveolin 1 are still present in a high density of 87 ± 23 particles per micrometre squared, again counted on six different areas within clusters of the caveolin label. The distribution of the caveolin label on the PF is dispersed (Fig. 6, inset); no more ring or circular structures can be found. However, the caveolin label is not totally randomly distributed. Clusters of 3–6 gold particles are often found at the periphery of intramembrane particle-free areas (Fig. 6, arrowheads). These more or less circular intramembrane particle-free domains (Fig. 6, asterisks) are still detectable after 30 min of cholesterol depletion.

When MßCD-treated 3T3 cells (15 or 30 min) are further grown for 1 day in normal MßCD-free serum containing culture medium, the process of caveolar flattening and re-distribution of caveolin is reversed (data not shown). The freeze-fracture morphology, structure and caveolin distribution of the caveolae did not differ significantly from that of cells without MßCD treatment given in Fig. 1.

Discussion

The morphology of caveolae viewed in electron micrographs has been known since the first ultrastructural descriptions of cells (Palade 1953; Yamada 1955), but the functions and dynamics of caveolae have not been explored until now. Compared with coated vesicles where the structure-determining coat protein clathrin exists (Pley and Parham 1993), in caveolae membrane lipids, such as cholesterol and sphingolipids together with oligomerised caveolin molecules form a structural framework (Rothberg et al. 1992; Murata et al. 1995). Caveolae are detergent-resistant membrane domains

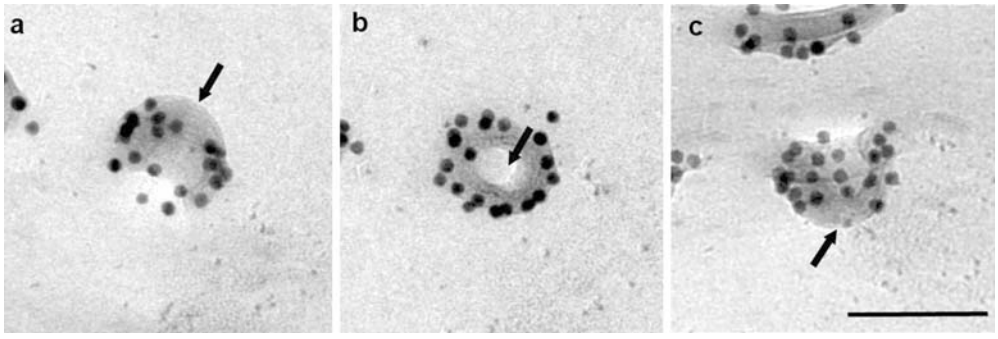

Fig. 3 Tilt series of one caveola with a dense label of caveolin 1 on the protoplasmic fracture face (PF) of 3T3-L1 mouse fibroblast cells. The micrograph shown in (**a**) is a −55° tilt view, in (**b**) a 0° view and in (**c**) a + 55° view. The tilt series shows that only the basolateral region of the caveola is labelled around with gold grains whereas the apical region (*black arrow*) is free of caveolin-1 labelling. For better visualisation of the carbon layer, an area of thin platinum decoration was chosen. *Bar*: 100 nm

(Brown and London 1998), which were found to depend on membrane cholesterol for preserving their structure and function. The aim of this work was to show the distribution of caveolin molecules in native plasma membrane caveolae of intact cells before and after depletion of membrane cholesterol. We applied methods of stereoscopic and tilt series image analysis to immunolabelled freeze-fracture replicas of caveolae. To our knowledge, this is the first time these methods have been applied. We found differences in caveolin-labelling patterns between deep and shallow caveolae. The great importance of stereoscopic analysis of freeze-fracture labelled samples has already been demonstrated by Rash and Yasumura (1999).

The cells used for the freeze-fracture labelling were cryofixed and not chemically fixed. Cryofixation is regarded as the most reliable method of preserving cellular ultrastructure without aggregation and shrinkage artefacts for electron microscopic analysis because it is both fast (milliseconds) and avoids the use of harmful chemicals on living cells (Dubochet and Satori Blanc 2001; Murk et al. 2003). After freeze-fracture analysis of chemically fixed cells most of the caveolar structures are fractured across their neck region, and the caveolar bulb is not replicated (Severs 1988; Westermann et al. 1999). Severs (1988) performed freeze-fracture preparation of chemically unfixed, directly frozen, endothelial plasma membranes. These unfixed preparations showed only a few caveolae fractured across their neck whereas in most cases, the caveolar vesicles were replicated. Severs (1988)

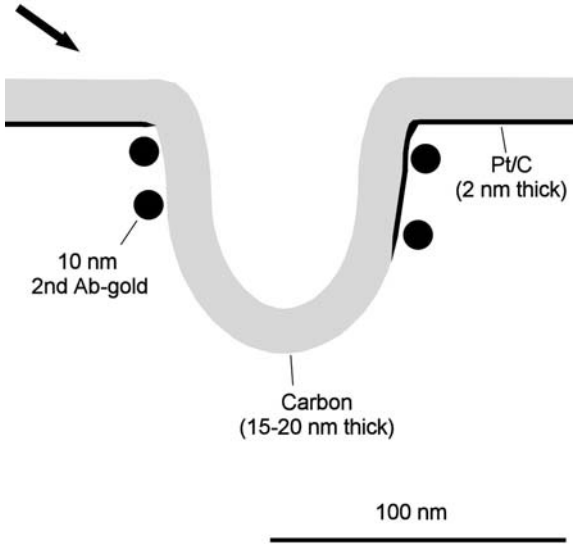

Fig. 4 A schematic cross-sectional view of a caveolin-1 immunolabelled freeze-facture replica of a deeply invaginated caveola. This model is drawn almost to scale and tries to summarise the data of the stereo and tilt analysis of caveolin-1 immunolabelled replica. The whole caveolar vesicle is replicated by the carbon layer whereas platinum/carbon (Pt/C) decorates only one side due to the 35° evaporation angle indicated by the *black arrow*. The caveolar opening is obviously not constricted. It has nearly the same diameter of about 80 nm like the vesicular invagination. The caveolin-1 label is found to surround the caveolar pit like a belt proximal to the plasma membrane whereas the apical region distal to the plasma membrane is nearly free of caveolin labelling

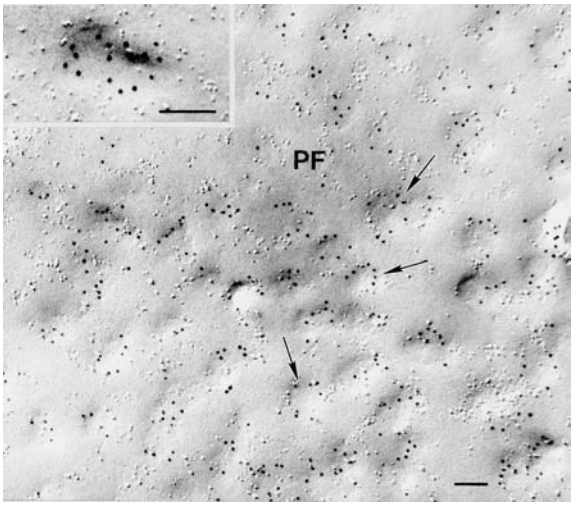

Fig. 5 Freeze-fracture immunolabelling of plasma membrane caveolin 1 in chemically unfixed 3T3-L1 mouse fibroblast cells. The cells were incubated for 15 min with 15 mM methyl-ß-cyclodextrin (MßCD) in culture medium. The protoplasmic fracture face (PF) was immunolabelled with caveolin-1 antibodies. The caveolar structures are flattened to dimensions of 80–110 nm in diameter. The gold particles indicating caveolin are found more dispersed in the periphery of shallow caveolar pits (*arrows*), often in a ring-like shape (*inset*). *Bar*: 100 nm

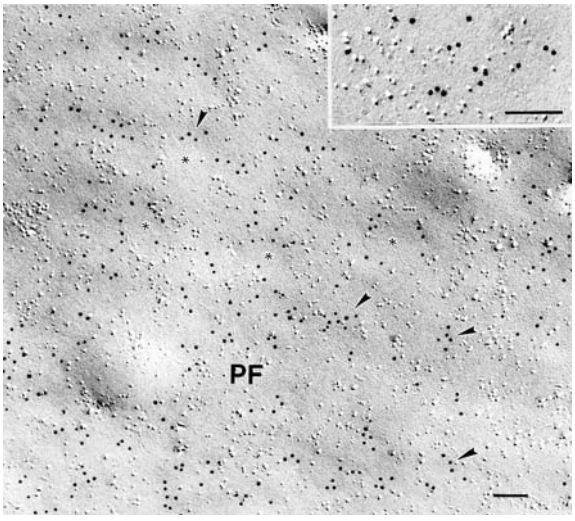

Fig. 6 Freeze-fracture immunolabelling of plasma membrane caveolin 1 in chemically unfixed 3T3-L1 mouse fibroblast cells. The cells were incubated for 30 min with 15 mM methyl-ß-cyclodextrin (MßCD). The caveolar pits on the protoplasmic fracture face (PF) are now flattened and decomposed. The PF is immunolabelled with caveolin-1 antibodies. Gold-labelled caveolin molecules are still found in the plasma membrane in a dispersed (*inset*) order. The caveolin label is not randomly distributed; clusters of 4–6 gold particles are often found (*arrowheads*) and flat intramembrane particle-free domains (*asterisks*) with dimensions of 80–110 nm in diameter remain. *Bars*: 100 nm

also found deep and shallow caveolae, which is a variation in the degree of invagination. His suggestion was that this variation represents different stages in vesicle formation and fusion. Similar data were shown by Fujimoto et al. (2000). They performed freeze-fracture labelling of caveolins and found that deeply invaginated caveolae were preferentially labelled by antibodies against the caveolin-1 isoform α over the shallow ones, indicating a different molecular composition of deep and shallow caveolae. Our stereoscopic and tilt series analysis showed that the total caveolar vesicle is replicated by the carbon layer whereas Pt/C only decorates one side due to the 35° evaporation angle used. The shape of replicated deeply invaginated caveolae in unfixed cells is not flask-like with a constricted neck region but more cup-like without a stricture below the basal opening (Fig. 4, schema).

The reason for the formation of a constriction at the caveolar opening after chemical fixation may be a cross-linking of proteins surrounding the caveolar opening, resulting in an artificial shrinkage in this area. Our results showed a belt-like caveolin-1 labelling basolateral at deeply invaginated caveolae whereas the apical region was almost free of caveolin labelling. Thorn et al. (2003) also localised caveolin 1 and 2 in TEM and SEM studies at the constricted neck region of caveolae in chemically fixed adipocytes. Circular arrangements of intramembrane protein particles surrounding the caveolar openings were shown by Westermann et al. (1999) on fracture images of deep caveolae in 3T3-L1 cells and on isolated caveolin-rich vesicles. They were also found by Severs and Simons (1986) surrounding the openings of caveolae in vascular smooth-muscle cells, and Oh et al. (1998) found dynamin rings at the neck of caveolae, mediating GTP-induced fission and budding of caveolae.

Our stereoscopic and tilt series results indicate in the case of unfixed cells a broad belt-like caveolin distribution at the basolateral part of deeply invaginated caveolae (Fig. 4, schema) instead of a ring-like or dispersed distribution, which was found in shallow caveolae or flattened caveolar domains after cholesterol depletion. There were observations of a "filamentous coat" attributed to spirally arranged caveolin-1 fibres covering the cytoplasmatic surface of caveolae (Peters et al. 1985; Rothberg et al. 1992). Fernandez et al. (2002) analysed the mechanism of caveolin filament assembly using recombinant caveolin. They proposed that α-helices of seven caveolin molecules through lateral interaction form oligomers 11 nm in diameter. These 11-nm sub-units are able to assemble to 50-nm-long filaments that match the morphology of the filaments of the caveolar coat. Analysing the caveolin immunogold label at deeply invaginated caveolae in 3T3 fibroblast cells (Figs. 1, 2, 3), we frequently found a broad belt of caveolin-1 indicating gold particles at the basolateral region of caveolae. The arrangement of caveolin coat filaments given in Rothberg et al. (1992) and Fernandez et al. (2002) is not completely in opposition to our findings. Two or three twists of 10-nm caveolin filaments covering the basolateral region of deep caveolae might cause this belt-like caveolin label. Furthermore, the rapid-freeze deep-etch micrographs (Rothberg et al. 1992) often show that 10-nm caveolin filaments do not cover the whole caveolar structure. Caveolin filaments spiral in two or three windings over the caveolar surface, but in some cases, especially after cholesterol depletion, they do not cover an area of 20–30 nm of the central part.

We used MßCD, a specific cholesterol-binding agent that—in contrast to nystatin or filipin—neither binds or inserts into the plasma membrane nor decreases the number of caveolae (Rothberg et al. 1990; Schnitzer et al. 1994). In contrast to Rothberg et al. (1992), our cholesterol-binding experiments were performed on living cells and not on isolated membrane fragments attached to a solid glass face. During the MßCD treatment of the cells, membrane components together with caveolin structures can move laterally freely in the plane of the membrane. Rothberg et al. (1992) found that the frequency of caveolin indicating the gold label on untreated rapid-freeze, deep-etched membranes was too low to determine positively whether the antibody was directly labelling the coat. They overcame the problem by incubating the membrane in the presence of nystatin to unravel the coat before applying the immunogold reagents. In contrast, the new freeze-fracture immunolabelling method showed high densities of caveolin labelling on untreated as well as cholesterol-reduced membranes of intact cells.

Our antibody is specific for the caveolin-1 isoforms α and ß and indicates a more or less dispersed caveolin

label on shallow caveolae in contrast to the distinct basolateral belts on deep caveolae. The function of these cholesterol-binding caveolin belts at deep caveolae may be the stabilisation of the membrane curvature and the segregation of caveolar lipids and proteins like a boundary zone from the surrounding bulk plasma membrane. It is assumed that lipids of caveolae form gel-like domains in the ''liquid-ordered'' phase state (Ahmed et al. 1997; Brown and London 1997), and it is known that sterol-containing model lipid systems in the ''liquid-ordered'' gel-phase state show membrane curvatures in dimensions of caveolar bulbs (Meyer et al. 1998). This suggests that caveolin indirectly causes the shape of deep caveolae and that the lipids, especially cholesterol, play an important role in caveolar structure formation.

When the cholesterol content is reduced by MßCD treatment, the caveolar membrane structure flattens, but the protein caveolin remains in the plasma membrane and the primary belt-like caveolin distribution in deep caveolae disintegrates to a ring-like and finally to a dispersed order. The obvious absence of intramembrane protein particles in freeze-fracture views of the caveolar bulb was already shown in longitudinally fractured caveolae (Severs 1988; Westermann et al. 1999). Our work exhibits the new finding that these particle-free domains remain and are still distinguishable from the bulk plasma membrane even after cholesterol depletion and caveolin redistribution. The remaining caveolin label is found in most cases at the periphery of the intramembrane protein-particle-free domains. In summary, the results indicate that cholesterol interacting with a belt of caveolin proteins at the basolateral region of caveolae is essential for the formation of deeply invaginated caveolar structures.

Acknowledgements We are grateful to Ms. M. Schilli-Westermann who did the cell culture. We also wish to thank Ms. I. Herrmann, Ms. R. Kaiser and Ms. C. Kämnitz for technical assistance and Ms. G. Engelhardt and Ms. G. Vöckler for their photographic work. The study was supported by the Deutsche Forschungsgemeinschaft (WE-2432/1-1).

References

Ahmed SN, Brown DA, London E (1997) On the origin of sphingolipid/cholesterol-rich detergent-insoluble cell membranes: physiological concentrations of cholesterol and sphingolipid induce formation of a detergent-insoluble, liquid ordered lipid phase in model membranes. Biochemistry 36:10944–10953

Anderson RG (1998) The caveolae membrane system. Annu Rev Biochem 67:199–225

Brown DA, London E (1997) Structure of detergent-resistant membrane domains: does phase separation occur in biological membranes? Biochem Biophys Res Commun 240:1–7

Brown DA, London E (1998) Functions of lipid rafts in biological membranes. Annu Rev Cell Dev Biol 14:111–136

Couet J, Li S, Okamoto T, Scherer P S, Lisanti MP (1997) Molecular and cellular biology of caveolae: paradoxes and plasticities. Trends Cardiovasc Med 7:103–110

Dietzen DJ, Hastings WR, Lubin DM (1995) Caveolin is palmitoylated on multiple cysteine residues. Palmitoylation is not necessary for localization of caveolin to caveolae. J Biol Chem 270:6838–6842

Dubochet J, Sartori Blanc N (2001) The cell in absence of aggregation artefacts. Micron 32:91–99

Dupree P, Parton RG, Raposo G Kurzchalia TV, Simons K (1993) Caveolae and sorting in trans-Golgi-network of epithelial cells. EMBO J 12:1597–1605

Fernandez I, Ying Y, Albanesi J, Anderson RG (2002) Mechanism of caveolin filament assembly. Proc Natl Acad Sci USA 99(17):11193–11898

Fra AM, Williamson E, Simons K, Parton RG (1995) De novo formation of caveolae in lymphocytes by expression of VIP21-caveolin. Proc Natl Acad Sci USA 92(19):8655–8659

Fujimoto K (1995) Freeze-fracture replica electron microscopy combined with SDS digestion for cytochemical labeling of integral membrane proteins. Application to the immunogold labeling of intercellular junctional complexes. J Cell Sci 108:3443–3449

Fujimoto K (1997) SDS-digested freeze-fracture replica labeling electron microscopy to study the two-dimensional distribution of integral membrane proteins and phospholipids in biomembranes: practical procedure, interpretation and application. Histochem Cell Biol 107(2):87–96

Fujimoto T, Kogo H, Nomura R, Une T (2000) Isoforms of caveolin-1 and caveolar structure. J Cell Sci 19:3509–35017

Hope HR, Pike LJ (1986) Phosphoinositides and phosphoinositide-utilizing enzymes in detergent-insoluble lipid domains. Mol Biol Cell 7:843–851

Irie T, Fukunaga K, Pitha JJ (1992) Hydroxypropylcyclodextrins in parenteral use. I: lipid dissolution and effects on lipid transfers in vitro. J Pharmacol Sci 81:521–523

Klein U, Gimpl G, Fahrenholz F (1995) Alteration of the myometrial plasma membrane cholesterol content with ß-cyclodextrin modulates the binding affinity of the oxytocin receptor. Biochemistry 34:13784–13793

Kurzchalia TV, Dupree P, Parton RG, Kellner R, Virta H, Lehnert M, Simons K (1992) VIP21, a 21KD membrane protein is an integral component of trans-Golgi network-derived transport vesicles. J Cell Biol 118:1003–1014

Kurzchalia TV, Parton RG (1996) And still they are moving ... Dynamic properties of caveolae. FEBS Lett 389:52–54

Li S, Couet J, Lisanti MP (1996) Src tyrosine kinases, Gα subunits, and H-Ras share a common membrane-anchored scaffolding protein, caveolin. Caveolin binding negatively regulates the auto-activation of Src tyrosine kinases. J Biol Chem 271:29182–29190

Meyer HW, Westermann M, Stumpf M, Richter W, Ulrich AS, Hoischen C (1998) Minimal radius of curvature of lipid bilayers in the gel phase state corresponds to the dimension of biomembrane structures ''caveolae''. J Struct Biol 124:77–87

Monier S, Parton RG, Vogel F, Henske A, Kurzchalia TV (1995) VIP21-caveolin, a membrane protein constituent of the caveolar coat, forms high molecular mass oligomers in vivo and in vitro. Mol Biol Cell 6:911–927

Montesano R, Roth J, Robert A, Orci L (1982) Non-coated membrane invaginations are involved in binding and internalization of cholera and tetanus toxins. Nature 296:651–653

Murata M, Kurzchalia T, Peranen J, Schreiner R, Wieland FT, Kurzchalia T, Simons K (1995) VIP21-caveolin is a cholesterol binding protein. Proc Natl Acad Sci USA 92:10339–10343

Murk JL, Posthuma G, Koster AJ, Geuze HJ, Verkleij AJ, Kleijmeer MJ, Humbel BM (2003) Influence of aldehyde fixation on the morphology of endosomes and lysosomes: quantitative analysis and electron tomography. J Microsc 212:81–90

Oh P, McIntosh DP, Schnitzer JE (1998) Dynamin at the neck of caveolae mediates their budding to form transport vesicles by GTP-driven fission from the plasma membrane of endothelium. J Cell Biol 141:101–114

Ohtani Y, Irie T, Uekama K, Fukunaga K, Pitha J (1989) Differential effects of alpha-, beta- and gamma-cyclodextrins on human erythrocytes. Eur J Biochem 186:17–22

Palade GE (1953) Fine structure of blood capillaries. J Appl Physics 24:1424

Parton RG (1994) Ultrastructural localization of gangliosides; GM1 is concentrated in caveolae. J Histochem Cytochem 42:155–166

Parton RG (1996) Caveolae and caveolins. Curr Opin Cell Biol 8:542–548

Parton RG, Joggerst B, Simons K (1994) Regulated internalisation of caveolae. J Cell Biol 127:1199–1215

Peters K-R, Carley WW, Palade GE (1985) Endothelial plasmalemmal vesicles have a characteristic striped bipolar surface structure. J Cell Biol 101:2233–2238

Pitha J, Irie T, Sklar PB, Nye JS (1988) Drug solubilizers to aid pharmacologists: amorphous cyclodextrin derivatives. Life Sci 43:493–502

Pley U, Parham P (1993) Clathrin: its role in receptor-mediated vesicular transport and specialized functions in neurons. Crit Rev Biochem Mol Biol 28:431–464

Rash JE, Yasumura T (1999) Direct immunogold labeling of connexins and aquaporin-4 in freeze-fracture replicas of liver, brain, and spinal cord: factors limiting quantitative analysis. Cell Tissue Res 296:307–321

Rothberg KG, Ying YS, Kamen BA, Anderson RG (1990) Cholesterol controls the clustering of the glycophospholipid-anchored membrane receptor for 5-methyltetrahydrofolate. J Cell Biol 11:2931–2938

Rothberg KG, Heuser JE, Donzell WC, Ying Y-S, Glenney JR, Anderson RGW (1992) Caveolin, a protein component of caveolae membrane coats. Cell 68:673–682

Sargiacomo M, Scherer PE, Tang ZL, Kübler E, Song KS, Sanders MC Lisanti MP (1995) Oligomeric structure of caveolin: Implications for caveolae membrane organisation. Proc Natl Acad Sci USA 92:9407–9411

Schnitzer JE, Oh P, McIntosh DP (1996) Role of GTP hydrolysis in fission of caveolae directly from plasma membranes. Science 274:239–242

Schnitzer JE, Oh P, Pinney E, Allard J (1994) Filipin-sensitive caveolae-mediated transport in endothelium: reduced transcytosis, scavenger endocytosis, and capillary permeability of select macromolecules. J Cell Biol 127:1217–1232

Schnitzer JE, Liu J, Oh P (1995) Endothelial caveolae have the molecular transport machinery for vesicle budding, docking, and fusion including VAMP, NSF, SNAP, annexins and GTPases. J Biol Chem 270:14399–14404

Severs NJ (1988) Caveolae: static inpocketings of the plasma membrane, dynamic vesicles or plain artifact? J Cell Sci 90:341–348

Severs NJ, Simons K (1986) Caveolar bands and the effects of sterol-binding agents in vascular smooth muscle cell plasma membrane. Single and double labeling with filipin and tomatin in the aorta, pulmonary artery and vena cava. Lab Invest 55:295–307

Simons K, Toomre D (2000) Lipid rafts and signal transduction. Nat Rev Mol Cell Biol 1:31–39

Stan RV (2002) Structure and function of endothelial caveolae. Microsc Res Tech 57(5):350–364

Takizawa T, Robinson JM (2000) Freeze-fracture cytochemistry: a new fracture-labeling method for topological analysis of biomembrane molecules. Histol Histopathol 15(2):515–522

Thorn H, Stenkula KG, Karlsson M, Ortegren U, Nystrom FH, Gustavsson J, Stralfors P (2003) Cell surface orifices of caveolae and localization of caveolin to the necks of caveolae in adipocytes. Mol Biol Cell 14(10):3967–3976

Westermann M, Leutbecher L, Meyer HW (1999) Membrane structure of caveolae and isolated caveolin-rich vesicles. Histochem Cell Biol 111:71–81

Yamada E (1955) The fine structure of the gall bladder epithelium of the mouse. J Biophys Biochem Cytol 1:445–458